



Resilience–throughput–power trade-off in future 5G photonic networks

Ákos Ladányi¹ · Tibor Cinkler¹

Received: 3 August 2018 / Accepted: 12 February 2019 / Published online: 23 March 2019
© The Author(s) 2019

Abstract

5G New Radio allows operators to use new and wider spectrum and complements Long-Term Evolution networks with higher data rates and lower latency. Supporting such requirements in the transport network is not only a technological challenge, but a financial one as well. The use of high-frequency or unlicensed spectrum and cell densification for capacity increases call for adoption of small cells. This means that the transport network needs to connect a large number of devices, which leads to high deployment costs. Improving resilience by redundancy would further inflate these cost. In this paper, we examine the prospect of enhancing resilience via an interleaved photonic transport network as well as by the cooperation of multiple operators. Resilience is quantified by the decrease in availability in case of a failure. Furthermore, we also investigate the case when the number of active cells is reduced not by failure, but due to deliberate switch-off in order to save power.

Keywords 5G · Resilience · Availability · Fixed-mobile convergence · Energy efficiency · Access networks · Photonic networks

1 Introduction

5G offers unprecedented technology options that enable the use of larger chunks of radio spectrum and provide major capacity and latency improvements. These capabilities enable new use cases like enhanced Mobile Broadband (MBB), Fixed Wireless Access (FWA) rivaling the speeds of wired solutions, massive and critical Internet of Things (IoT) services, automotive and manufacturing applications.

The transport network plays a critical role in realizing these advancements. Several technologies are considered for this role, e.g., point-to-point fiber access, Passive Optical Network (PON), Flexible Ethernet, and Optical Transport Network (OTN) [1]. Among these, PON stands out as a strong contender due to its point-to-multipoint topology,

efficient use of fiber resources and already widespread use for wireline broadband access.

PONs are point-to-multipoint fiber-optic access networks. They employ unpowered optical splitters to serve multiple endpoints. A PON consists of an Optical Line Terminal (OLT), which is at the service provider's premises, and of multiple Optical Network Units (ONUs), which are located at the consumers end. The OLT is connected to the splitter through optical fiber, and then, the splitter is connected to the ONUs. Downstream signals are broadcast to all ONUs and encryption is used to prevent access to data that is not intended for a given endpoint. Upstream transmission is handled using multiple access protocols, usually Time Division Multiple Access (TDMA).

In this work, we evaluate a hybrid access network architecture which consists of a wireless small cell network and a PON which serves as the backhaul connection for the cells.

Small cells are low-powered, close to mid range radio access nodes. They enable tighter spatial reuse through cell densification, and thus are a key instrument of system capacity improvement. Mobile operators can also use them to extend service coverage in indoor or rural deployments. Some 5G features like the utilization of high-frequency spectrum (due to propagation) or the use of unlicensed

✉ Ákos Ladányi
ladanyi@tmit.bme.hu

Tibor Cinkler
cinkler@tmit.bme.hu

¹ High-Speed Networks Laboratory (HSNLab), Department of Telecommunications and Media Informatics, Budapest University of Technology and Economics, Magyar tudósok körútja 2, Budapest 1117, Hungary

spectrum (due to transmit power regulations) also imply the use of small cells.

Deployment costs are only one side of the coin. A significant part of operating costs are related to energy consumption. It is estimated that access networks are responsible for 70% of the total energy consumption of telecommunication networks [2]. Therefore, energy efficient access networks can result in major savings. Both cells and ONUs are capable of entering a low-power state for idle periods. In case of ONUs proposals to the IEEE 802.3av task force have been made to standardize this mode of operation [3].

1.1 Contribution

This work investigates the triple trade-off between availability, power consumption, and Quality of Service (QoS). The first scenario we evaluate is a hybrid access network consisting of a small cell network and a wireline PON backhaul. Two orthogonal possibilities are investigated: switching off cells voluntarily to save power, and losing part of the cellular network due to failure of the underlying PON. Both of these lead to a reduced number of active cells and can have a negative effect on the QoS and the availability of network services. We examine how the PON topology can be adapted to alleviate these negative effects.

In the second scenario, a similar small cell network is evaluated in presence of multiple operators. The possible savings in power consumption and service availability benefits of more than one operator’s network providing coverage to the same area are examined.

1.2 Related work

Several previously published papers cover partially the topic of this one. References [4, 5] investigate a similar hybrid wireless-optical access network, the main difference being the wireless part is a multi-hop wireless mesh network and backhaul failures are not investigated. Reference [6] also investigates a hybrid access network consisting of a PON and Wireless Fidelity (Wi-Fi). It focuses on the trade-off between throughput and power consumption. Reference [7] analyzes the QoS in an Long-Term Evolution (LTE) access network combined with different optical backhaul solutions. Reference [8] considers selective switch-off with a focus on transients between states. Energy efficiency in the context of PONs is investigated in [9, 10]. Network sharing solutions with a focus on indoor and local area provisioning are compared from a business model standpoint in [11]. A similar approach is chosen in [12, 13], but the authors consider macrocells. A multi-operator deployment problem is investigated in [14] for indoor picocells. In [15], a multi-operator game-theoretic cell switch-off method is evaluated with the aim of reducing power consumption. This method has the

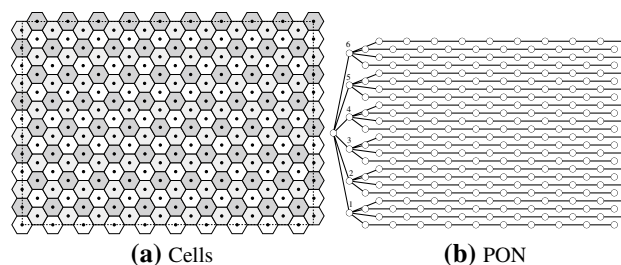


Fig. 1 Scenario

advantage that it does not require exchanging information between operators. In [16], the authors investigate the cell switch-off problem and propose a reinforcement learning based scheme to deal with the dynamic traffic load. [17] proposes an algorithm for selecting cells to switch-off during low traffic hours where neighboring cells increase their transmit power to cover the area of inactive ones. Reference [18] proposes a multi-operator cooperative switch-off heuristic which select cells and reassigns User Equipments (UEs) respecting their QoS requirements.

2 System model

2.1 Network architecture

Figure 1 shows the main scenario evaluated in this work. Figure 1a illustrates the wireless part. This consists of 24 rows (henceforth streets) with 10 cells in each. That is 240 cells in a regular hexagonal grid.

Figure 1b illustrates the PON connecting the cells to the core network. The leftmost node represents a 6 port OLT. The 6 direct neighbors of this node represent the 6 splitters. The rest of the nodes are ONUs which connect the cells to the PON. Each OLT port serves 4 streets, that is 40 ONUs/cells. The fibers leading from a splitter to a given ONU are not depicted separately for visual clarity.

2.2 Wireless network definition

Without the loss of generality, we use an LTE model here. A 5G New Radio model would result in higher throughput values, and different power consumption, but would not alter the general findings.

Let us define an LTE network as a set of:

- cells $\mathcal{C} = \{C_1, \dots, C_m, C_n, \dots, C_C\}$,
- users per cell $\mathcal{U} = \{U_1, \dots, U_u, \dots, U_U\}$,
- Resource Blocks (RBs) $\mathcal{K} = \{1, \dots, k, \dots, K\}$,
- Modulation and Coding Schemes (MCSs) $\mathcal{R} = \{1, \dots, r, \dots, R\}$ (Table 1).

Table 1 MCS (modulation and coding schemes)[19]

MCS	Modulation	Code rate	SINR threshold (dB)	Efficiency
MCS1	QPSK	1/12	− 6.50	0.15
MCS2	QPSK	1/9	− 4.00	0.23
MCS3	QPSK	1/6	− 2.60	0.38
MCS4	QPSK	1/3	− 1.00	0.60
MCS5	QPSK	1/2	1.00	0.88
MCS6	QPSK	3/5	3.00	1.18
MCS7	16QAM	1/3	6.60	1.48
MCS8	16QAM	1/2	10.00	1.91
MCS9	16QAM	3/5	11.40	2.41
MCS10	64QAM	1/2	11.80	2.73
MCS11	64QAM	1/2	13.00	3.32
MCS12	64QAM	3/5	13.80	3.90
MCS13	64QAM	3/4	15.60	4.52
MCS14	64QAM	5/6	16.80	5.12
MCS15	64QAM	11/12	17.60	5.55

2.2.1 Network assumptions

For the sake of simplicity, assumptions have been made, which do not involve any loss of generality when assessing the performance of the system:

1. A full buffer model is used to simulate the traffic of users, i.e., there is always data available to be transmitted for all users [20].
2. A perfectly synchronized Orthogonal Frequency Division Multiple Access (OFDMA) network is assumed. In this way, inter-cell interference will occur only when more users are allocated to the same RB at the same time in different cells.
3. The coherence bandwidth of the channel is larger than the bandwidth of an RB. In this case, the fading of all subcarriers within an RB is the same.
4. The coherence time of the channel is larger than the time duration of an RB. In this case, the fading of all OFDM symbols within an RB is equal.

2.2.2 Signal quality

The Signal to Interference plus Noise Ratio (SINR) $\gamma_{u,k}$ of user u in RB k is modeled as:

$$\gamma_{u,k} = \frac{P_{u,k}^m \cdot \Gamma_{m,u}}{w_{u,k} + \sigma^2} = \frac{P_{u,k}^m \cdot \Gamma_{m,u}}{\sum_{m'=1, m' \neq m}^C P_{u',k}^{m'} \cdot \Gamma_{m',u} + \sigma^2} \tag{1}$$

where $P_{u,k}^m$ denotes the power applied by C_m in each one of the subcarriers of RB k , in which user u is allocated. $\Gamma_{m,u}$ is

the channel gain between cell C_m and user u . $w_{u,k}$ represents the received signal strength, i.e., interference, suffered by user u in RB k . Finally, σ is the density of noise.

2.2.3 User capacity

The bit rate $BR_{u,r,k}$ as well as the throughput $TP_{u,r,k}$ of user u in RB k when using MCS r are modeled as:

$$BR_{u,r,k} = \Theta \cdot eff_r = \frac{SC_{ofdm} \cdot SY_{ofdm}}{T_{subframe}} \cdot eff_r \tag{2}$$

$$TP_{u,r,k} = BR_{u,r,k} \cdot (1 - BLER(r, \gamma_{u,k})) \tag{3}$$

where Θ is a fixed parameter that depends on network configuration, being SC_{ofdm} and SY_{ofdm} the number of data subcarriers (frequency) and symbols (time) per RB, respectively, and $T_{subframe}$ is the RB duration in time units. Moreover, eff_r is the efficiency (*bits / symbol*) of the selected MCS r , while $BLER(r, \gamma_{u,k})$ indicates the BLock Error Rate (BLER) suffered by RB k , which is function of both r and $\gamma_{u,k}$ ¹.

Let us note that using a set of MCSs is a more realistic approach than using the theoretical Shannon’s capacity [21]. This is because in a real system not only the user SINR determines its bit rate, but also the efficiency of its MCS. When using Shannon’s formula a larger SINR is always translated into a larger bit rate, but not when utilizing MCSs. For example, in this case (Table 1), an SINR ≥ 17.6 dB always leads to a bit rate equal to 732.6 kbps per RB (Eq. 2).

3 Impact of optical topology

In this section, we investigate the impact of reduced active cell numbers on the service availability and throughput experienced by the UEs and the sum power consumption of the network. Cells can become inactive either because of deliberate switch-off (in order to save power), or due to a failure in the PON network connecting the cells to the OLT.

3.1 Selective switch-off and consolidation

We devised two switch-off strategies for comparison. The objective of these is to turn off currently dispensable cells to save power. These might not be practical as is, but demonstrate the possible achievements of such methods.

The first strategy, named Power Saving (PS), periodically (every 10 s) checks for each cell if for some UE the given

¹ The BLER is generally computed using Link-Level Simulations (LLSs) and is made available to the System-Level Simulations (SLSs) through Look Up Tables (LUTs). In this case, we took the LUTs of [19].

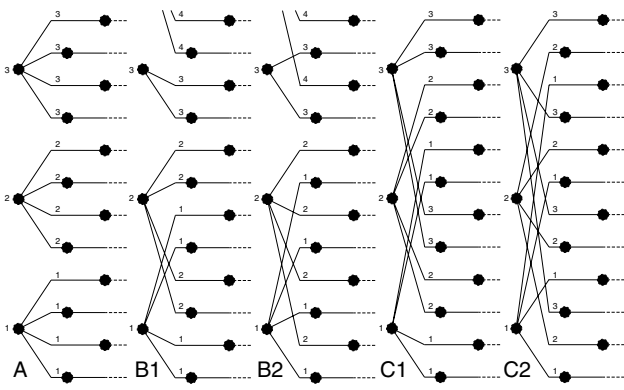


Fig. 2 PON topologies

cell is the closest one. In case there is such a UE, the cell becomes (or stays) active, otherwise it gets turned off. In other words, this method tries to deactivate those cells which would not be selected as best server by any UE.

The second strategy is based on the set covering problem (SCP) [22]. Here, the objective is to select a minimum number of cells so that all UEs are covered by at least one cell.

$$\min \sum_{c \in \mathcal{C}} x_c \tag{4a}$$

subject to:

$$\sum_{c: u \in \mathcal{U}_c} x_c \geq 1 \quad \forall u \in \mathcal{U} \tag{4b}$$

$$x_c \in \{0, 1\} \quad \forall c \in \mathcal{C} \tag{4c}$$

where \mathcal{C} is the set of cells, \mathcal{U} is the set of UEs, and \mathcal{U}_c is the set of UEs inside the coverage area of cell c .

This optimization problem is solved periodically (every 10 s), and the cells corresponding to the minimum covering sets are kept active, the others are switched off.

3.2 PON tree failure

The failure of a tree in the PON network causes the failure of a large number of cells. To mitigate the effects of this, the PON trees can be formed in such a way that the cells of a single tree are spatially distributed. That is, even if a tree fails and therefore a given number of cells fail, at least they shall be spread out, and not concentrated to the same area.

Besides the simplest solution (named topology “A”) depicted in Fig. 1b, we evaluated four others. Figure 2 shows the scheme in which the streets are assigned to OLT ports. Note that the figure shows only the first cell of each street, and only the bottom 12 streets.

- In topology “A” 4 neighboring streets are connected to the same OLT port. This will be a worst-case scenario,

since in case a tree fails, all the affected cells are in the same rectangular area.

- In topology “B1” the streets are assigned to OLT ports in blocks of two, where a block consists of two neighboring streets. Then every second block is connected to the same OLT port.
- In topology “B2” every second street is connected to the same OLT port.
- In topology “C1” the streets are assigned to OLT ports in blocks of two, where a block consists of two neighboring streets. Then every third block is connected to the same OLT port.
- In topology “C2” every third street is connected to the same OLT port.

There is not a significant difference in cost between these topologies since they only differ in the segments connecting the splitter and the streets, which is a relatively small part of the whole PON.

3.3 Evaluation

This section presents a performance analysis regarding power consumption, throughput and availability of the previously described access network instance.

The scenario used for evaluation is deployed over an area of 1.892 km². The scenario covers 24 vertical streets with 10 cells in each. The distance between two cells in a street is 173.21 m. The distance between neighboring streets is 50 m.

Users are placed uniformly distributed within the scenario area and move along random waypoints according to a pedestrian mobility model based on [23]. The simulations were done with 30, 100 and 300 UEs in the scenario. A full buffer model is used to simulate the traffic of users, i.e., there is always data available to be transmitted for a user. Furthermore, all users have a throughput demand of 2 Mbps.

Only downlink transmission is simulated. We applied a Frequency Reuse Scheme (FRS) of 3, that is each eNodeB is restricted to a third of the available frequency resources. Inside this one-third band round-robin scheduling is used to assign RBs to the UEs. More details about the dynamic SLS tool used for this experimental evaluation can be found in [24]. The simulation parameters and scenario are presented in Table 2 and Fig. 1, respectively. Path loss was modeled according to the COST Hata model [25], and slow fading was also considered using a log-normal shadowing with a standard deviation of 8 dB. Furthermore, subframe errors were modeled based on BLER LUTs obtained from LLSs [19].

In this case, 10 min of network functioning was simulated. Samples of power consumption, throughput, availability and other indicators were taken every 10 s.

Table 2 Simulation parameters

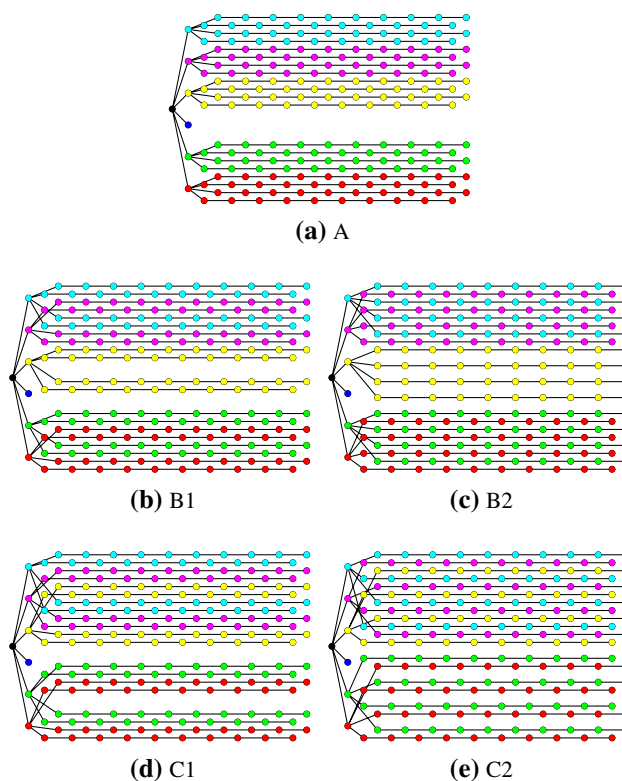
Parameter	Value
#eNodeBs	240
Sectors per eNodeB	1
Site-to-site distance	173.21 m
Carrier frequency	2.0 GHz
Channel bandwidth	5 MHz
Duplexing	FDD
Frame duration	1 ms
RBs	25
OFDM data symbols	11
BS Tx power	30 dBm
BS ant. pattern	Omni
BS ant. height	4 m
BS noise figure	5 dB
BS cable loss	3 dB
UE ant. gain	0 dBi
UE ant. pattern	Omni
UE ant. height	1.5 m
UE noise figure	9 dB
UE body loss	0 dB
Type of service	Full buffer
Min service BR	2 Mbps
Shadowing s.d.	8 dB
Correl. shadow. dist.	50 m
Intra BS correl.	1.0
Inter BS correl.	0.5
Path loss model	COST Hata
User distribution	Uniform
FRS	Reuse 3

Table 3 Device power consumption [26]

Device	Active (W)	Inactive (W)
eNodeB	14.7	4.3
ONU	10	1

When calculating the power consumption, we assume that when switching off a cell then the corresponding ONU is set to the inactive state as well. We also assume that when a PON tree fails the affected ONUs and cells enter the inactive state. The power consumption of each network element can be found in Table 3. Note that in this paper the terms inactive state, sleep state, and switched off are used as synonyms. They indicate a state of the device, in which it does not perform its usual function, but consumes less energy, and is able to recover from fairly quickly.

When evaluating the effect of a failed PON tree, we assume that the failed tree is the one rooted at the 3rd splitter (counting from below; see Figs. 1b, 3). A cable cut between

**Fig. 3** PON topologies after tree failure

the OLT and the splitter or an OLT port failure results in such a tree failure.

3.3.1 Availability

The availability of a UE reflects the probability that it can connect to the access network and through it reach the core network. It can be calculated for a given UE at a given location based on which cells are in its range, and the availability of the network elements (cell, ONU, fiber to the splitter, splitter, fiber to the OLT, OLT) which constitute the paths leading to the core network (the upstream port of the OLT in our model). Assuming a UE at a given location we first determine which cells are in its range. Then, we build a graph where an edge is added between the node representing the UE and the cells which are in range. The rest of the graph corresponds to the physical topology connecting the cell to the core network through the PON components. From the availability of the network components we can calculate the availability experienced by the UE because the network components are either connected in series or parallel.

The more cells the UE can connect to, the higher the resulting availability. If these cells are failure-independent (connect to different PON trees), that further improves the availability.

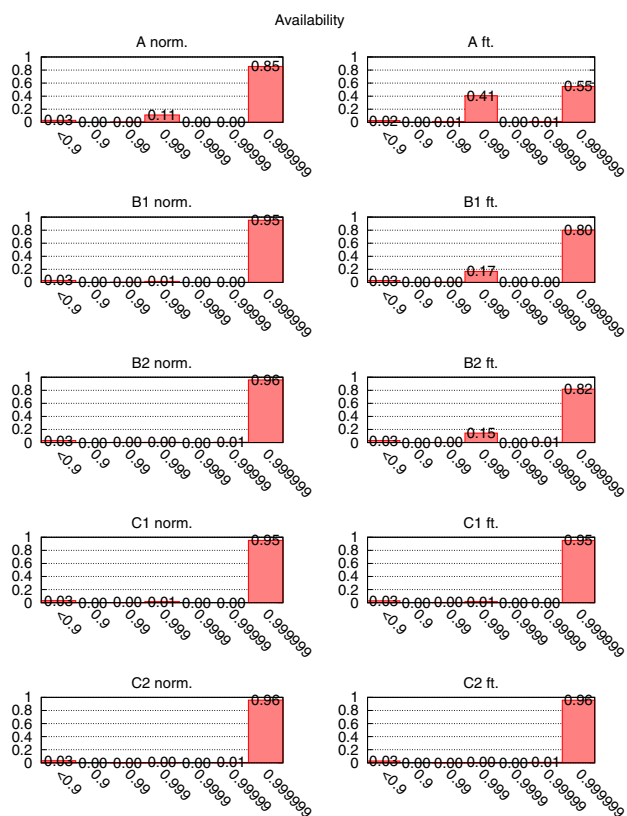


Fig. 4 Availability versus PON topology (300 UEs)

During the simulation, we calculate an availability value for each UE every 10 s. The distribution of the availability values obtained this way can be seen in Fig. 4. It is to be noted, that if a UE can only connect to cells of a single tree, then its availability will be around 0.999 (“three nines”). In case it can connect to at least two trees, it can achieve an availability of 0.999999 (“six nines”).

Figure 4 shows how the availability depends on the PON topology in case the network is in working condition (norm.) and if there is a failed PON tree (ft.). This figure shows the results for 300 UEs, but the results for 30 or 100 UEs are very close to these. This is because the UE count affects only the number of availability samples taken. In case there is no failure, only topology “A” shows lower than 0.999999 availability for a significant percentage of samples. This is because large continuous areas are covered by the same PON tree. In case of the rest of the topologies, the UEs are able to connect to at least two trees. This changes when one of the trees fails (ft. cases). The availability for “A” gets worse, and it decreases for both “B1” and “B2” too, while for “C1” and “C2” it is unaffected. This can be explained by the properties of topology “C1” and “C2”. For these, the areas of the failed streets are always surrounded by different trees both from the “south” and the “north”. This is not always true for

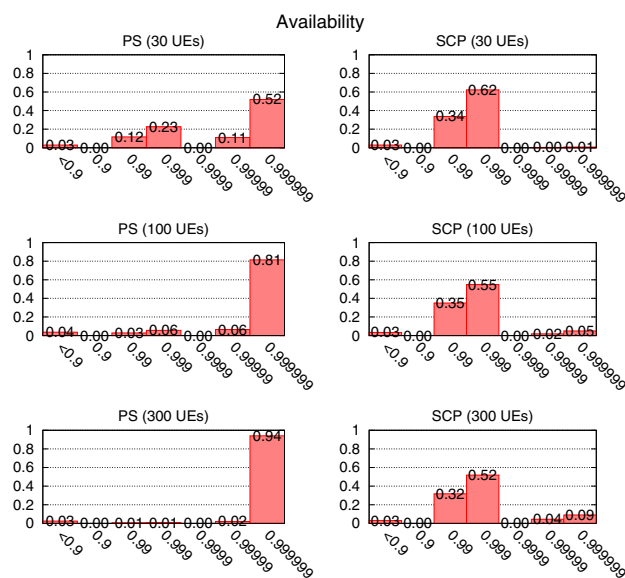


Fig. 5 Availability versus selective switch-off (topology “C2”)

“B1” and “B2”. While topology “A” has this favorable property, the area affected by the failure is just too wide.

The selective switch-off schemes also influence the availability, since they reduce the number of active cells. Figure 5 shows the availability distribution for the PS and SCP schemes with varying number of UEs in the scenario. The numbers for the “C2” topology are shown here. This topology was chosen, because it is one with the least impact on the availability due to the distributed nature of its trees.

In case of SCP, the availability distribution peeks at, and before 0.999. This is a consequence of SCP trying to thin out coverage as much as possible. That is it covers the set of UEs with a minimum number of cells. This causes that most UEs are covered by one cell or by cells of the same tree.

The results also indicate that PS turns off less cells, than SCP, which is in line with the power consumption figures.

In case of the PS method, it is true that with the increase of the user population the algorithm has less and less impact on the availability. This is because with more users in the scenario less cells can be turned off, since there is a higher chance that some UE will be close by. Furthermore, the PS method has a smaller impact on availability regardless of user population, due to keeping more cells active compared to SCP.

In case, the PON tree failure happens when one of the selective switch-off algorithms is enabled, the availability is affected similarly to the case without the failure. The impact of the tree failure and that of the switch-off on the availability accumulates, but the trends remain the same.

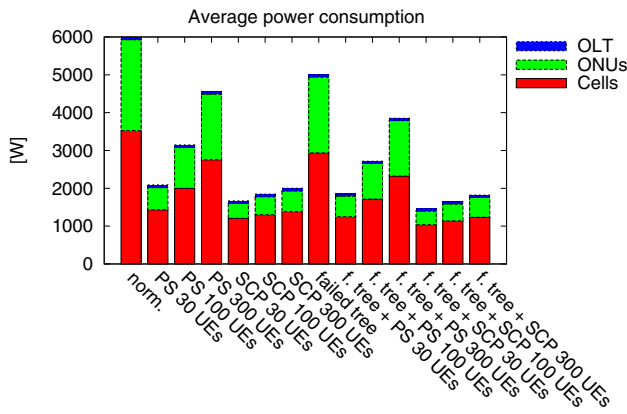


Fig. 6 Average power consumption

3.3.2 Power consumption

Figure 6 shows the average power consumption. The first bar shows the case when there is no failure and also no selective switch-off. This yields the maximum power consumption, since every device is always turned on.

The next three bars show the power consumption with the PS selective switch-off method enabled. Here, the power consumption depends on the number of UEs in the scenario, since having more UEs decreases the chance that a cell can be turned off.

The next three bars show the results with the SCP selective switch-off method enabled. Again, the values increase with the number of UEs because more cells are needed to cover a larger set of UEs. This method yields even lower power consumption than the PS, since PS keeps the closest cell active for each UE, while SCP just ensures that all UEs are in the coverage of some cell, thus keeps less cells active. In other words, the solution that PS yields satisfies constraints (4b) and (4c), but does not guarantee a minimum number of active cells (assuming all UEs are in the coverage area of some cell, which is the case here).

The 8th bar (failed tree) shows the case, when a PON tree failed, so 40 cells of the 240 are cut off, but no selective switch-off algorithm was enabled. The power consumption decreases proportionally to the number of lost cells.

The last 6 bars show the results of the selective switch-off algorithms, while there is a failed tree. The trend regarding the number of UEs is the same as before, while the slightly lower values compared to the cases with no failure are explained by the missing 40 cells. Note that these last 6 bars are for topology “A”. The results for the other topologies are very close to these, so they are not depicted. The reason for this is that the topology determines which cells fail, and in a few cases this changes which cells get switched off.

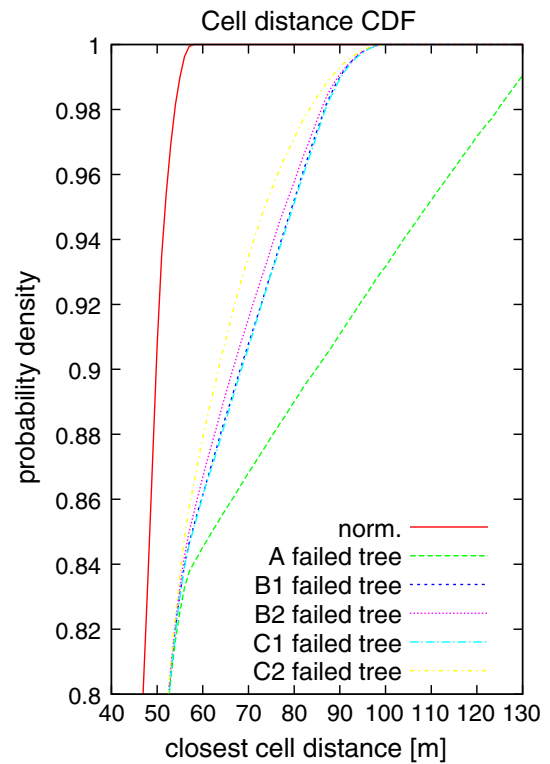


Fig. 7 Distance to the closest cell

3.3.3 Distance to the closest cell

Figure 7 shows the Cumulative Distribution Function (CDF) of the distance to the closest cell. This is an important measure, since closer serving cell means a stronger carrier signal. The failure of a PON tree essentially removes a lot of cells, thus on average it increases the distance to the closest cell. As one can see the increase is the highest in case of scenario “A” compared to the case without failure (norm.), because here the cells of four neighboring streets fail. For the other four scenarios, the distance increases too compared to the case with no failure, but the difference between them is not significant. However the two leftmost curves of these are topologies “B2” and “C2”, because in these none of the failed streets are neighbors.

3.3.4 Cell area

In this context, area of a cell means those points of the scenario from which the closest cell is the given cell. This is approximately the area in which the UEs select the given cell as their server. The size of this area is an important factor, since the bigger it is, the more users are likely to be served by the cell. More users can mean that the cell gets overloaded.

Table 4 Cell area

Cell area (1000 m ²)	Norm.	Failed tree				
		A	B1	B2	C1	C2
2–3	2	2	2	2	2	2
4–5	40	32	30	29	28	18
5–6	0	2	2	4	4	12
6–7	0	0	0	0	0	6
7–8	0	0	2	0	4	0
8–9	198	126	110	102	90	81
10–11	0	18	18	18	36	9
11–12	0	0	0	18	0	18
12–13	0	2	0	0	0	22
13–14	0	0	0	0	0	32
14–15	0	0	0	0	0	0
15–16	0	0	18	0	36	0
16–17	0	0	0	0	0	0
17–18	0	0	18	27	0	0
24–25	0	18	0	0	0	0
Total	240	200	200	200	200	200

Table 4 shows the distribution of the cell areas. The first column shows the case without failure. The meaning of the values is that there are 2 cells with an area between 2000 m² and 3000 m², there are 4 cells with an area between 4000 m² and 5000 m², and there are 198 cells with an area between 8000 m² and 9000 m². The total row contains 240, because there are 240 cells in the scenario altogether. The next five columns show the cases with a failed PON tree for the different PON topologies. The total row contains 200 in these columns, because 40 cells are affected by the failure.

In case there is no failure, the area of most of the cells is around 8000 m². The cells around the border of the scenario have an approximate area of 4000 m², while the ones in the bottom left and top right corner have around 2000 m².

A failure causes that 40 cells “disappear.” The ones close to these will serve the UEs of the failed ones. That is the area of cells close to the failed ones increases. This holds true for all five PON topologies, but affects them to different degrees depending on the spatial distribution of the failed cells.

PON topology “A” is a worst case: after failure 18 cells have an area around 24000 m². This is because the cells of four neighboring streets fail, and the cells of the street to the south and to the north need to serve the affected area (Fig. 3a).

PON topologies “B1”, “B2” and “C1” are hard to tell apart based on this measure. “B1” (Fig. 3b) and “C1” (Fig. 3d) suffer from increased cell areas, because there are neighboring streets among the failed ones. While topology “B2” (Fig. 3c) is unfavorable because the failed streets are separated by only one street of working cells. Topology “C2” (Fig. 3e) does not suffer from any of the mentioned flaws, and this reflects in that the largest cell area here is

between 13000 and 14000 m², which, compared to the previous three topologies, is significantly lower.

3.3.5 PON load after tree failure

The distribution of the traffic load among the remaining PON trees in case of a failure also depends on the topology. The remaining trees might get overloaded in case, e.g., only one or few of them need to carry the additional traffic in case of a failure.

A way to quantify this property is to check which trees the streets next to the failed ones belong to. In these calculations we assume that the immediate neighbors of a failed street share the extra load equally. For example, in case of topology “C1,” the lower two failed streets are between tree no. 1 (red) and no. 2 (green). The two streets account for half of the load, so tree no. 1 gets 1 / 4 and tree no. 2 gets 1 / 4 too. Tree no. 2 and tree no. 4 (yellow) share similarly the load of the other failed two streets, that is no.

Table 5 Neighboring trees of the failed one

Topology	Traffic distribution to working trees
A	2 (1/2), 4 (1/2)
B1	2 (1/4), 4 (3/4)
B2	2 (1/8), 4 (7/8)
C1	1 (1/4), 2 (1/2), 3 (1/4)
C2	1 (3/8), 2 (1/2), 3 (1/8)

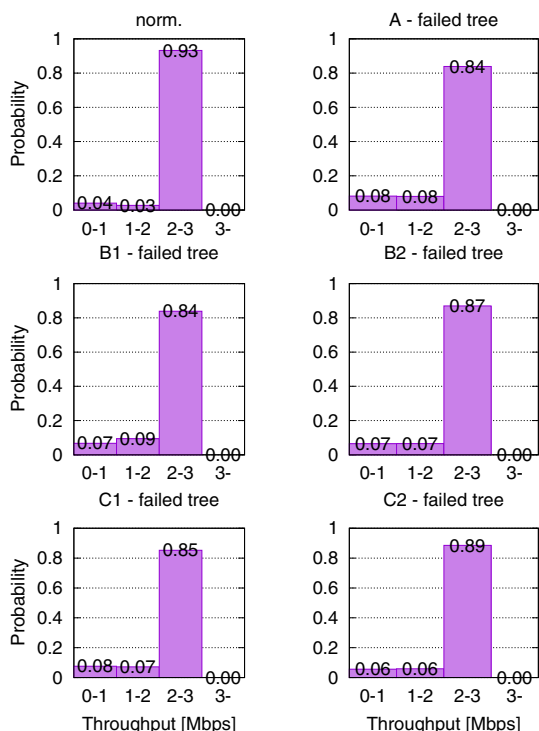


Fig. 8 Throughput versus PON topology (100 UEs)

2 gets 1 / 4 and no. 4 gets 1 / 4. In total tree no. 1 gets 1 / 4, no. 2 gets 2 / 4, and no. 4 gets 1 / 4.

Table 5 shows which trees will carry additional traffic in case of a failure. The values in the parentheses indicate what portion of the additional traffic the tree will need to carry in case of a failure. In case of topology “A,” the traffic of a failed tree gets distributed between two trees equally (no. 2 and no. 4). In case of topology “B1” and “B2,” the excess traffic is distributed between the same two trees, but not in a balanced way. Most of it is carried by tree no. 4. In case of topologies “C1” and “C2,” the traffic is distributed among three trees: no. 1, 2 and 4. In case of “C1,” the ratio is more balanced than in case of “C2”.

Considering the distribution of the extra traffic created by the failure topologies “C1” and “C2” seem to be the most favorable.

3.3.6 Throughput

The throughput samples were generated by calculating the throughput of each UE every 10 s in the simulation using the calculation outlined in Sect. 2.2.3.

Figure 8 shows the effect of a PON tree failure on the throughput for different topologies. While the difference not being substantial, topologies “B2” and “C2” are the least affected. These are the only two topologies, where the failed

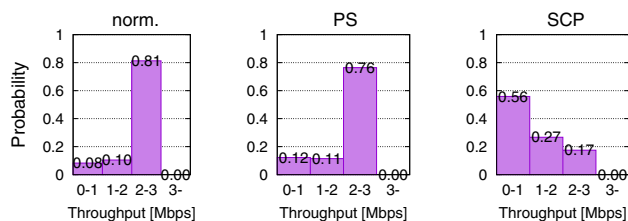


Fig. 9 Throughput versus selective switch-off (100 UEs, topology “C2”)

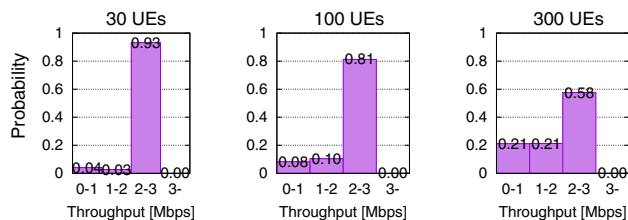


Fig. 10 Throughput versus number of UEs (no failure, topology “A”)

streets are never neighbors. Also this is in line with the closest cell distance distribution discussed previously.

Figure 9 shows the impact of the selective switch-off algorithms on the throughput. The PS method has a slight to none effect on the throughput, because its target is to keep the cell closest to the UE active. While the SCP method severely limits the throughput due to taking into account only that the UE is in the coverage area of the cell, which can leave many UEs at cell edges. The effect of the PS and SCP methods on the throughput remains the same even if there is a failed tree in the network.

Figure 10 shows how the number of UEs affects the throughput. As expected, with the growing number of UEs, less and less of them has its 2 Mbps demand satisfied.

The systems capacity may seem to be low. However, one needs to keep in mind that the simulations were done assuming a 5 MHz LTE network, moreover the reuse 3 scheme further reduces the usable bandwidth. The parameters were calibrated intentionally so that reaching the systems limits does not require the simulation of an excessive amount of UEs.

4 Impact of operator coordination

Up until this point we investigated the impact of the optical topology, here we look at the advantages and disadvantages resulting in from multiple operators coordinating selective switch-off and consolidation. We assume that 2–4 operators are providing service in the same area. Each operator’s network consists of 5 LTE small cells. Figure 11 shows the evaluated scenario. There are 5 cell locations in it. All operators

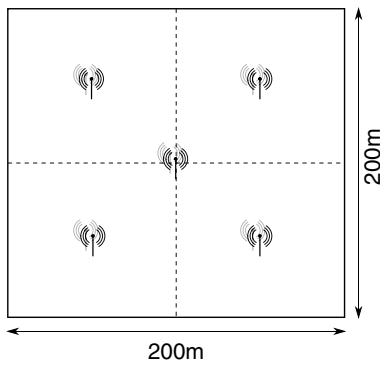


Fig. 11 Multi-operator scenario

have one cell at each location. That is altogether there are 10 cells in case of 2 operators, 15 in case of 3 and 20 in case of 4. We also assume that all networks use different frequency bands, that is cells of different operators do not interfere.

One can argue that such arrangements are wasteful, but the presence of more than one operator is required to avoid monopoly, and separate infrastructure and spectral band per operator is also not unheard-of (and prevalent at least in macro scenarios).

All UEs in the scenario belong to a given operator. The UEs can connect to their operator’s network without restriction. They can also connect other operator’s network, but their resource usage is limited. The case when this limit is zero is also considered, which correspond to the case when UEs can only use their own operator’s network (no roaming). Varying levels (0–100%) of this resource sharing limit is evaluated in our simulations.

From the operator’s point of view, we will refer to the UEs of the operator as ‘own’ and to the UEs of the other operator as ‘foreign’.

4.1 Selective switch-off and consolidation

We assume that the operators employ a coordinated strategy to turn off unneeded cells to minimize the power consumption of their network. We use the following method to simulate this. The method is based on an assignment problem. It tries to assign each UE to a cell in a way that the throughput demand of each UE is satisfied. For each UE-cell pair, it calculates how many RBs would it take to satisfy a given throughput demand if the UE would be served by the given cell.

$$\min \sum_{\forall j} y_j - K \sum_{\forall i} \sum_{\forall j} x_{ij} \tag{5a}$$

subject to:

$$x_{ij} \in \{0, 1\} \quad y_j \in \{0, 1\} \quad i \in \mathcal{U} \quad j \in \mathcal{C} \tag{5b}$$

$$y_j \geq x_{ij} \quad \forall i \in \mathcal{U} \quad \forall j \in \mathcal{C} \tag{5c}$$

Table 6 Simulation parameters

Parameter	Value
#eNodeBs	10; 15; 20
Channel bandwidth	20 MHz
RBs	100
BS Tx power	31 dBm
BS ant. height	3 m
Min service BR	1-5 Mbps

$$\sum_{\forall i} x_{ij} \geq y_j \quad \forall j \in \mathcal{C} \tag{5d}$$

$$\sum_{\forall j} x_{ij} \leq 1 \quad \forall i \in \mathcal{U} \tag{5e}$$

$$\sum_{\forall i} x_{ij} D_{ij} \leq R \quad \forall j \in \mathcal{C} \tag{5f}$$

$$\sum_{\forall i \in \mathcal{F}_j} x_{ij} D_{ij} \leq L \quad \forall j \in \mathcal{C} \tag{5g}$$

where \mathcal{U} is the set of UEs, \mathcal{C} is the set of cells, \mathcal{F}_j is the set of UEs foreign to cell j ($\mathcal{F}_j \subset \mathcal{U}$), R is the number of resource blocks, L is the number of resource block allowed for foreign UEs ($L \leq R$), D_{ij} is the number of resource blocks required by user i if connected to cell j , and K is a large enough number so that the second sum dominates the objective (in our case $K = 100$). Variable x_{ij} indicates whether UE i is assigned to cell j , or not. Variable y_j indicates whether cell j is turned on or off. The objective is to assign the maximum number of UEs to cells while minimizing the number of needed active cells (Eq. 5a). Equation (5c) ensures that if at least one UE is assigned to a cell, then it is turned on. Equation (5d) ensures that if no UEs are assigned to a cell, then it is turned off. Equation (5e) ensures that each UE is assigned to at most one cell. Equation (5f) states that connected UEs cannot use more resources than available, while Eq. (5g) ensures that foreign UEs do not get more resources than a given limit (L). The method has a parameter, which is the throughput which it tries to allocate for all UEs. The value of this parameter influences the calculation of D_{ij} .

This optimization problem is solved periodically. The result of the optimization is the set of cells which are kept active, the rest is turned off.

This approach can be thought of as a refined version of the SCP method (Sect. 3.1) since it not only ensures coverage for each UE, but also guarantees a minimum throughput.

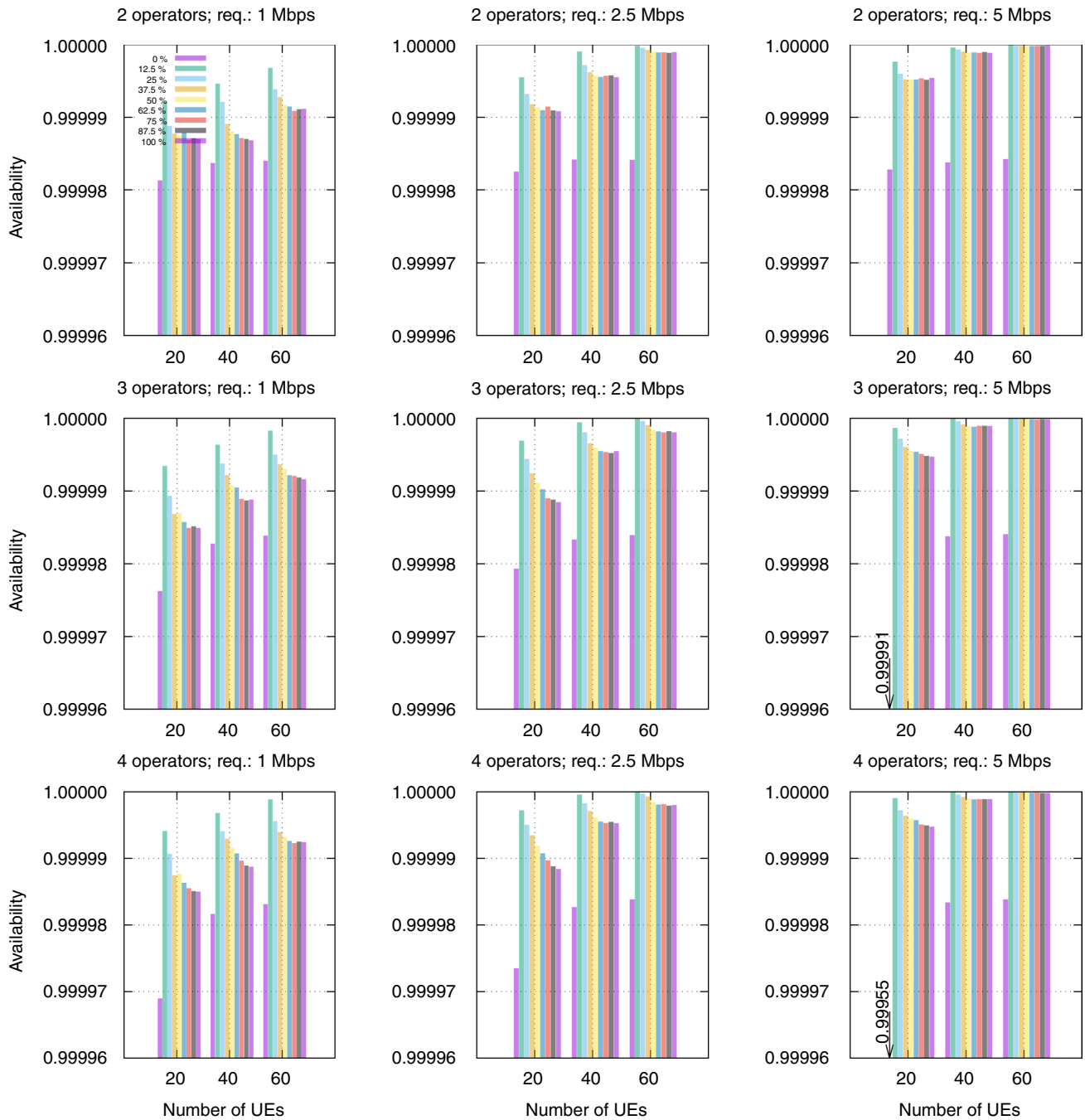


Fig. 12 Availability with multiple operators

4.2 Evaluation

The scenario used for evaluation is deployed over an area of 40.000 m² (a square with sides of 200 m). The traffic model, user distribution and mobility model is the same as used in Sect. 3.3. Table 6 shows the simulation parameters which are different from the ones used previously

(Table 2). As before 10 min of are simulated, moreover throughput and availability samples are taken every 10 s for each UE. Unless noted, otherwise any simulation detail is the same as used in the first set of experiments.

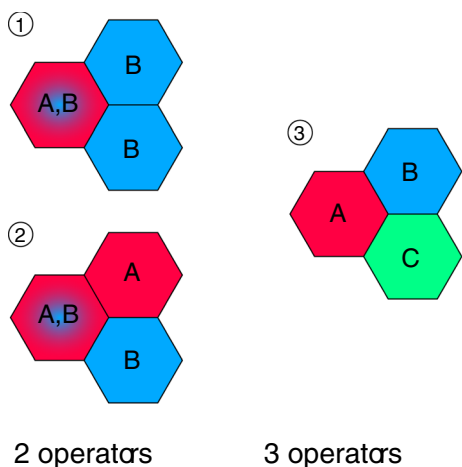


Fig. 13 2 Versus 3 operators

4.2.1 Availability

The service availability for a UE is calculated the same way as before with the extension that in case the assignment algorithm is not able to select a cell for the UE, then its availability is zero. In every subfigure of Fig. 12, a given column shows the average of all availability samples collected during the simulation with the given number of UEs and given value of the resource sharing limit (L). The color of the bars corresponds to the resource sharing limit. The bar groups inside a given subfigure correspond to the number of UEs in the scenario area (20, 40, 60). Among the multiple subfigures the rows show the results for a given number of operators (2, 3, 4), while the columns show it for different UE throughput requirements (1 Mbps, 2.5 Mbps, 5 Mbps). All operators get equal number of own UEs, for example in case of 60 UEs and 3 operators each operator has 20 own UEs.

Availability is always worse if UEs are not allowed to use foreign networks (0% case) compared to when there is some level of resource sharing. Without resource sharing,

only the cells of the UE’s own network are available as connection points.

If there is resource sharing, the more resources we allow for foreign UEs, the more the availability decreases. With more resource sharing the total the number of required cells decreases, thus the availability decreases.

Factors which increase the required capacity, like the number of UEs or their throughput demand, increase the number of required active cells, and thus improve the availability.

The number of operators has a more complex effect on the availability. In some cases, more operators improve the availability, while in some cases degrade it.

On the one hand, more operators mean more possible connection points for a UE, which improves the availability. On the other hand since cells of different operators do not interfere, more operators can reduce the overall interference, thus improve cell capacity, which can mean that less cells are needed to cover the UE population, which decreases availability. Figure 13 shows an example for such a situation (A, B and C are the operators). Assuming that the leftmost hexagonal area has more UEs than the other two, and thus requires the cell of two operators (A and B) to be active, while in the other areas one is enough. With 2 operators there are two possible cases, in which one or both leftmost cells get interfered by their neighbors. With 3 operators it is possible to cover the area with 3 cells in such a manner, that neither interferes the other. Thus, due to the reduced interference 3 cells can be enough instead of 4.

If there is no resource sharing among operators, then the availability decreases with the number of operators, because the number of own UEs per operator decreases, thus the required number of active cells decreases, while each operator’s network does not affect the network of others in any way (no interference, no resource sharing).

With low levels of resource sharing, the increased number of available cells is the significant factor and the additional capacity provided by foreign cells is small thus the availability increases. With high levels of resource sharing, the additional

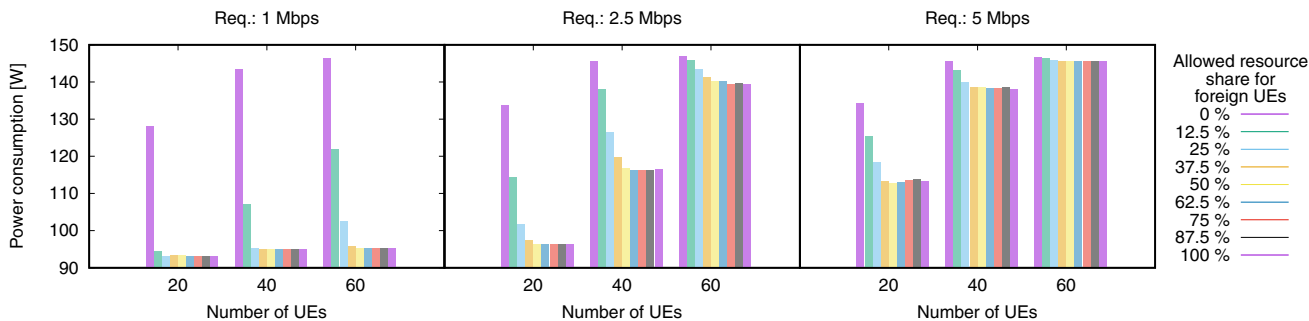


Fig. 14 Power consumption (two functioning networks)

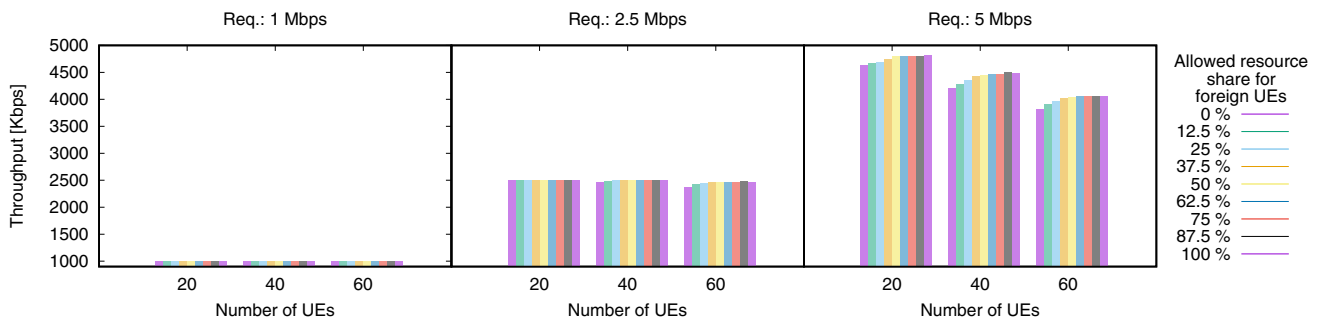


Fig. 15 Throughput (two functioning networks)

foreign cell capacity is significant, thus the number of required cells decreases, which negatively influences the availability.

4.2.2 Power consumption and throughput

In this section, we concentrate on the 2 operator case, and a variant of it where one of the two networks failed. The methodology is similar as before. The number of UEs in the scenario area varies (20, 40, 60). Half of them belong to the first operator, the other half to the second. The throughput requirement of the UEs also changes. The third varying parameter is the allowed resource share for foreign UEs (p). This is the percentage of the RBs that can be allocated to them (see Eq. (5); $L = p/100 * R$).

Figure 14 shows how the total power consumption of all cells changes with the above-mentioned parameters. It increases with the load—either due to more UEs or the higher throughput requirement since more cells are required. With 60 UEs and 5 Mbps requirement all cells are turned on most of the time. The more resources are allowed for foreign UEs the less the required total power becomes. This is because the more the UEs of the two operators are allowed to share, the less the required number of cells becomes. As one can see the most significant savings can be achieved when the network utilization is low.

Figure 15 shows the average throughput of the UEs. As one can see without resource sharing ($p = 0%$), the UEs can achieve their required throughput only when the network load is low (requirement is 1 Mbps or 2.5 Mbps and the number of UEs is 20). It is noteworthy that higher levels of resource sharing is also beneficial to the achievable throughput. With 60 UEs and a requirement of 5 Mbps network capacity becomes a bottleneck.

Now we look at a modified scenario, where one of the two networks has failed. The UEs of this network are only able to connect through the network of the other operator, thus they suffer from both the resource usage restriction applied to foreign UEs and the reduced total capacity (5 cells instead of 10). In these simulations, the number of UEs was 40, and

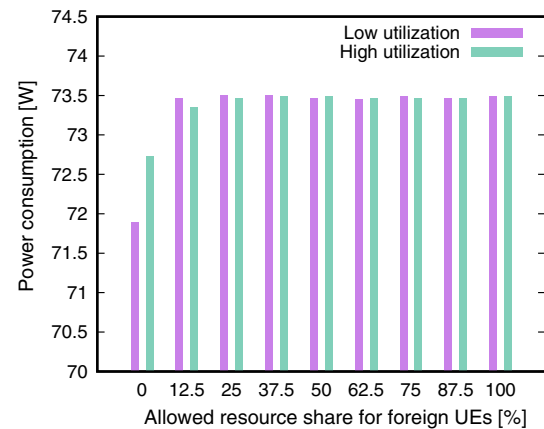


Fig. 16 Power consumption with a failed network

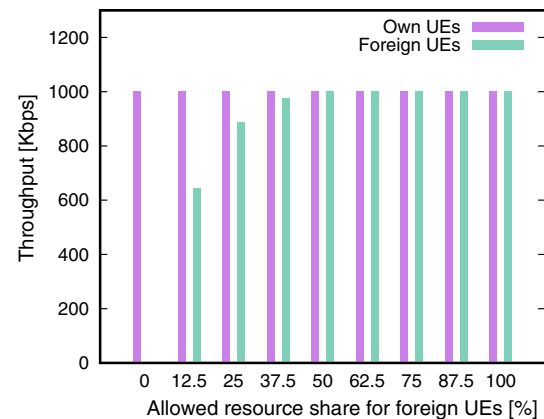


Fig. 17 Throughput with a failed network (low utilization)

the throughput requirement of each was either 1 Mbps (for the low utilization case), or 5 Mbps (for the high utilization case).

Figure 16 shows the total power consumption of the operational network in the low and high utilization case (we assume that the failed cells do not require any power). In both cases, the power consumption increases with the

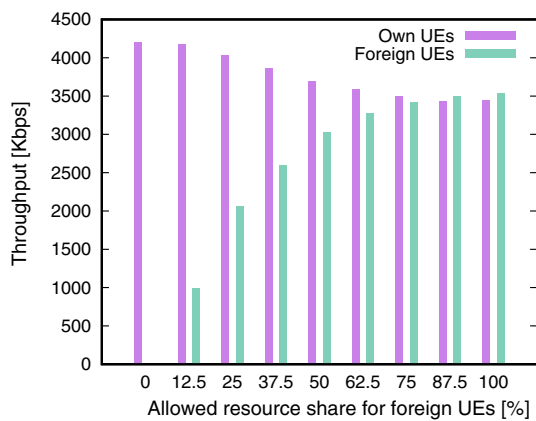


Fig. 18 Throughput with a failed network (high utilization)

allowed resource share, since this means that more traffic is let into the network, and thus more active cells are needed. The power consumption is generally high, which is explained by the relatively numerous UE population and the reduced number of available cells.

Figure 17 shows the average throughput when the network utilization is low (requirement is 1 Mbps). In this context, own UEs are the UEs of the operator with the functioning network, foreign UEs are the UEs of the operator with the failed network. Here, the throughput of own UEs is unaffected by the increasing resource share of foreign UEs, since the network’s capacity is high enough to serve both.

Figure 18 shows the average throughput when the network utilization is high (requirement is 5 Mbps). With the increase in the foreign UE resource limit, the throughput of them increases as expected. At the same time the throughput of own UEs decreases, since the foreign ones occupy more and more resources, and there is not enough capacity for both groups.

5 Conclusion

The results of the system-level simulations show the following evidence about the implications of selective switch-off techniques, the choice of PON topologies and the benefits of multiple operators:

PON topologies with spatially distributed and interleaved trees can help achieving higher availability and better excess load distribution for both cells and PON trees.

When applying selective switch-off algorithms, it is not enough to consider UE locations on the level of whether they are within the coverage area of a cell or not. Turning off cells so that many UEs are left on cell edges is detrimental to service quality.

The availability is more susceptible to cells disappearing (either due to failure or switch-off) than the throughput.

Various benefits can come from operators coordinating the shutdown of unneeded cells and allowing restricted access to the UEs of others. At times, when the utilization is low, significant power savings can be achieved. Moreover, such coordination between operators also enables the mitigation of total service outage in case of extensive failures.

Acknowledgments Open access funding provided by Budapest University of Technology and Economics (BME).

Open Access This article is distributed under the terms of the Creative Commons Attribution 4.0 International License (<http://creativecommons.org/licenses/by/4.0/>), which permits unrestricted use, distribution, and reproduction in any medium, provided you give appropriate credit to the original author(s) and the source, provide a link to the Creative Commons license, and indicate if changes were made.

References

1. Wey, J.S., Zhang, J.: Passive optical networks for 5G transport: technology and standards. *J. Lightwave Technol.* <https://ieeexplore.ieee.org/document/8412589/> (2018)
2. Lange, C., Gladisch, A.: On the energy consumption of FTTH access networks. In: OFC/NFOEC, San Diego, CA, USA (2009)
3. Mandin, J.: EPON powersaving via sleep mode. http://www.ieee802.org/3/av/public/2008_09/3av_0809_mandin_4.pdf (2008)
4. Chowdhury, P., Mukherjee, B., Sarkar, S., Kramer, G., Dixit, S.: Hybrid wireless-optical broadband access network (WOBAN): prototype development and research challenges. *IEEE Netw.* **23**(3), 41–48 (2009)
5. Chowdhury, P., Tornatore, M., Sarkar, S., Mukherjee, B.: Building a green wireless-optical broadband access network (WOBAN). *J. Lightwave Technol.* **28**(16), 2219–2229 (2010)
6. Togashi, K., Nishiyama, H., Kato, N., Ujikawa, H., Suzuki, K.-I., Yoshimoto, N.: On the effect of cooperation between power saving mechanisms in WLANs and PONs. In: ICC-2013, Budapest, Hungary (2013)
7. Giuntini, M., Valenti, A., Matera, F., Di Bartolo, S.: Quality of service management in hybrid optical-LTE access networks. *Future Netw. Mob. Summit (FutureNetw)* **2011**, 1–7 (2011)
8. Conte, A., Feki, A., Chiaraviglio, L., Ciullo, D., Meo, M., Marsan, M.A.: Cell wilting and blossoming for energy efficiency. *IEEE Wirel. Commun.* **18**(5), 50–57 (2011)
9. Shah Newaz, S.H., Cuevas, Á., Lee, G.M., Crespi, N., Choi, J.K.: Adaptive delay-aware energy efficient TDM-PON. *Comput. Netw.* **57**(7), 1577–1596 (2013)
10. Zhang, L., Yu, C., Guo, L., Liu, Y.: Energy-saving mechanism based on double-sleep-state algorithm and dynamic double-threshold receiver selection in EPON. *Optik Int. J. Light Electron Opt.* **124**(18), 3655–3664 (2013)
11. Markendahl, J., Ghanbari, A.: Shared smallcell networks. In: The 4th International Workshop on Indoor and Outdoor Small Cells, Tsukuba Science City, Japan (2013)
12. Beckman, C., Smith, G.: Shared networks: making wireless communication affordable. *Wirel. Commun.* **12**(2), 78–85 (2005)
13. Khan, A., Kellerer, W., Kozu, K., Yabusaki, M.: Network sharing in the next mobile network: TCO reduction, management flexibility, and operational independence. *IEEE Communi. Mag.* **49**(10), 134–142 (2011)
14. Gatzoulis, L., Povey, G., Band, I., Wilson, D.: Indoor FDD multi-operator deployment. In: 4th International Conference on 4th

- International Conference on 3G Mobile Communication Technologies, 2003. 3G 2003(Conf. Publ. No. 494), pp. 37–41 (2003)
15. Antonopoulos, A., Kartsakli, E., Bousia, A., Alonso, L., Verikoukis, C.: Energy-efficient infrastructure sharing in multi-operator mobile networks. *IEEE Commun. Mag.* **53**(5), 242–249 (2015)
 16. Li, R., Zhao, Z., Chen, X., Palicot, J., Zhang, H.: Tact: a transfer actor-critic learning framework for energy saving in cellular radio access networks. *IEEE Trans. Wirel. Commun.* **13**(4), 2000–2011 (2014)
 17. Bousia, A., Antonopoulos, A., Alonso, L., Verikoukis, C.: “green” distance-aware base station sleeping algorithm in lte-advanced. In: 2012 IEEE International Conference on Communications (ICC), pp. 1347–1351 (2012)
 18. Oikonomakou, M., Antonopoulos, A., Alonso, L., Verikoukis, C.: Cooperative base station switching off in multi-operator shared heterogeneous network. In: 2015 IEEE Global Communications Conference (GLOBECOM), pp. 1–6 (2015)
 19. Forsk SARL. Forsk Atoll—global RF planning solution. http://www.forsk.com/htm/products/atoll_overview.htm, (2009) Accessed: 2009 Sept 24
 20. Necker, M.: Interference coordination in cellular OFDMA networks. *IEEE Netw.* **22**(6), 12–19 (2008)
 21. Shannon, C.E.: Communication in the presence of noise. *Proc. Inst. Radio Eng.* **37**(1), 10–21 (1949)
 22. Vazirani, V.V.: *Approximation Algorithms*. Springer, Berlin (2001)
 23. Bettstetter, C.: Smooth is better than sharp: a random mobility model for simulation of wireless networks. In: Proceedings of the 4th ACM International Workshop on Modeling, Analysis and Simulation of Wireless and Mobile Systems, pp. 19–27, Rome, Italy (2001)
 24. López-Pérez, D., Ladányi, Á., Jüttner, A., Zhang, J.: OFDMA femtocells: a self-organizing approach for frequency assignment. In: IEEE Personal, Indoor and Mobile Radio Communications Symposium (PIMRC), Tokyo, Japan (2009)
 25. Directorate-General for the Information Society and Media (European Commission). COST Action 231 Final Report. (1999)
 26. Powerlib. <http://powerlib.intec.ugent.be/>, Accessed: 2012 Sept 10 (2012)

Publisher’s Note Springer Nature remains neutral with regard to jurisdictional claims in published maps and institutional affiliations.



Ákos Ladányi has received M.Sc. (2006) degree from the Budapest University of Technology and Economics, Hungary, where he also conducted his Ph.D. studies at the Department of Telecommunications and Media Informatics. He spent 2 years at the University of Bedfordshire as an exchange Ph.D. student. His research interests include routing, resilience, traffic engineering in multi-layer optical networks, resource allocation and self-organization in cellular networks.



Tibor Cinkler has received M.Sc. in 1994 and Ph.D. in 1999 degrees from the Budapest University of Technology and Economics (BME), Hungary, where he is currently associate professor at the Department of Telecommunications and Media Informatics (TMIT). His research interests focus on optimization of routing, traffic engineering, design, configuration, dimensioning and resilience of IP, Ethernet, MPLS, ngSDH,

OTN and particularly of heterogeneous GMPLS-controlled WDM-based multi-layer networks. He is author of over 200 refereed scientific publications and of four patents. He has been involved in numerous related European and Hungarian projects including ACTS METON and DEMON; COST 266, 291, 293; IP NOBEL I and II and MUSE; NoE e-Photon/ONe, e-Photon/ONe+ and BONE; CELTIC PROMISE and TIGER2; NKFP, GVOP, ETIK; and he has been member of ONDM, DRCN, BroadNets, AccessNets, IEEE ICC and Globecom, EUNICE, CHINACOM, Networks, WynSys, ICTON, etc. Scientific and Programme Committees. He has been guest editor of a Feature Topic of the IEEE ComMag and reviewer for many journals. He has organized DRCN 2001, ONDM 2003 and Networks 2008 conferences in Budapest. He teaches various courses on networking and optimization at the university, as well as for companies and also gives tutorials at conferences and summer and winter schools. He received numerous awards including: Dimitris Chorafas Prize for Engineering, ICC best paper award, numerous HTE awards (HTE is the Hungarian IEEE sister society), including Tivadar Puskás, Virág-Pollák 3 times, and the 60-year anniversary medal Bolyai Medal, etc.